CAUCHY – Jurnal Matematika Murni dan Aplikasi
Volume 11 (1) (2026), Pages 350-363
p-ISSN: 2086-0382; e-ISSN: 2477-3344

# Stability Analysis of a Three-Trophic Rice Ecosystem with Holling Type II and Crowley–Martin Responses

Anastasya Choirun Nisa' and Dian Savitri*

*Department of Mathematics, Universitas Negeri Surabaya, Surabaya 60292, Indonesia*

**Abstract**

This study examines three-trophic-level ecological dynamics in rice field ecosystems involving rice as the producer, brown planthoppers (*Nilaparvata lugens*) as herbivores, and *Pardosa* sp. as top predators. Population interactions were modeled using logistic growth for rice and two response functions: the Holling type II response for planthopper predation on rice, and the Crowley–Martin response for *Pardosa* sp. predation on planthoppers to capture predator interference. The resulting model was formulated as a system of nonlinear differential equations. Analytically, four equilibrium points were obtained: total population extinction, extinction of planthoppers and *Pardosa* sp., extinction of *Pardosa* sp., and coexistence of all three species. Local stability analysis at each equilibrium point was conducted using the Jacobian matrix and the Routh–Hurwitz criterion. Numerical simulations were performed for several parameter combinations by varying planthopper growth efficiency and *Pardosa* sp. predation intensity. Parameter values are obtained from relevant literature where available, and the remaining parameters are considered reasonable biological assumptions for exploring the dynamics of the system qualitatively. The simulation results were consistent with the theoretical analysis and showed that small changes in biological parameters could shift the system from stable coexistence to near extinction of the planthopper population. Ecologically, the model demonstrates that rice field ecosystem balance is strongly influenced by the interaction between planthopper reproductive capacity and the predatory strength of *Pardosa* sp., providing theoretical insights that may support the development of sustainable planthopper pest management strategies.

**Keywords:** Holling type II functional response; Crowley–Martin functional response; three-trophic food chain; rice field ecosystem



## 1. Introduction

In rice field ecosystems, a three-tier trophic system consists of rice plants as producers, brown planthoppers (*Nilaparvata lugens*) as herbivores, and *Pardosa* sp. as top predators. These three components form an ecosystem and are closely related to maintaining the stability of rice field ecosystems. An imbalance in one trophic level can trigger pest outbreaks and cause cascading declines in other trophic levels [1]. Therefore, studying and understanding the dynamics of interactions between the three trophic levels is crucial for designing strategies for sustainable and environmentally friendly rice field ecosystem stability [2].

*Corresponding author. E-mail: diansavitri@unesa.ac.id

Submitted: January 06, 2026 Reviewed: January 13, 2026 Accepted: February 17, 2026
DOI: https://doi.org/10.18860/cauchy.v11i1.40204

Mathematical modeling can be used to study complex relationships in a three-trophic-level rice field ecosystem involving producers, herbivores, and carnivores that act as natural predators. By using dynamical models and testing various biological parameters such as growth rates, consumption levels, and predation efficiency on system stability, the analysis allows for predicting ecological system dynamics and long-term outcomes [3]. Such tri-trophic food chain models have been widely applied to investigate coexistence, extinction, and complex oscillatory behavior in ecological systems [1, 4, 5]. Similar three-species prey–predator–super predator frameworks have also been studied with Holling-type functional responses and shown to exhibit Hopf bifurcation and oscillatory dynamics under parameter variation [6].

In prey–predator ecological dynamics, the response function serves to link the predator's consumption rate with prey density, thereby becoming a key factor in determining the stability of the ecological system [2, 7]. One of the most widely used functional responses is the Holling type II response, which incorporates the concept of handling time, defined as the time required for predators to capture and consume prey [8, 9, 10, 11]. This functional form produces a nonlinear relationship in which consumption increases rapidly at low prey densities but saturates when predators are limited by handling capacity [12, 13]. Consequently, the Holling type II response is suitable for describing herbivore–plant interactions, such as the relationship between rice plants and brown planthoppers in two-trophic systems [14].

In ecological modeling, predator interference refers to a reduction in individual predation efficiency caused by interactions among predators, such as competition, disturbance, or mutual obstruction during the hunting process [7, 15]. Unlike prey-dependent functional responses, interference-based responses explicitly incorporate predator density into the functional form, leading to decreased per capita consumption as predator density increases [2, 16]. Among such formulations, the Crowley–Martin functional response accounts for predator interference by allowing predator density to influence both searching and handling processes, making it particularly suitable for modeling active hunting predators such as *Pardosa* sp. [15, 17].

Several functional responses have been proposed to incorporate the effects of predator interference, among which the Beddington–DeAngelis and Crowley–Martin formulations are the most widely used. The Beddington–DeAngelis functional response assumes that predator interference primarily affects predator search efficiency, while handling time remains independent of predator density [16, 18]. In contrast, the Crowley–Martin functional response allows predator interference to affect both search and handling processes, resulting in a stronger nonlinear dependence on predator density [4, 15]. Recent studies have shown that this formulation can generate more complex and ecologically realistic dynamics in multi-trophic food web models, particularly when predator density plays a significant role in predation efficiency [1, 17].

Despite extensive developments in three-trophic food chain models, most existing studies focus on single functional responses or do not explicitly analyze the role of predator interference at the upper trophic level in determining the stability of coexistence equilibria [1, 4]. In particular, analytical conditions for the existence and local stability of interior equilibrium points under the Crowley–Martin functional response remain limited, especially in the context of rice field ecosystems [17]. Motivated by this gap, this study develops a three-trophic ecological model that integrates the Holling type II functional response at the producer–herbivore level and the Crowley–Martin functional response at the herbivore–predator level. The main contribution of this work lies in deriving equilibrium conditions and local stability criteria using the Jacobian matrix and the Routh–Hurwitz approach, complemented by numerical simulations to illustrate how variations in biological parameters affect long-term ecosystem dynamics.

## 2. Methods

This section outlines the methodological framework adopted in this study, including the literature review, model formulation, equilibrium analysis, and stability assessment used to investigate the proposed tri-trophic system.

### 2.1. Literature study

This study begins with a literature study on predator–prey and tri-trophic ecological models, particularly those applied to agricultural and rice field ecosystems. Previous works discussing Holling type II functional responses are reviewed to understand herbivore–plant interactions, while studies employing the Crowley–Martin functional response are examined to capture predator interference effects. The reviewed literature provides the theoretical foundation for selecting appropriate functional responses, defining model assumptions, and determining biologically meaningful parameter ranges used in this research.

### 2.2. Model construction

Based on the literature review, a three-trophic-level ecological model is constructed to represent interactions among rice plants as producers, brown planthoppers (*Nilaparvata lugens*) as herbivores, and *Pardosa* sp. as top predators in rice field ecosystems. The rice population is assumed to grow logistically, reflecting limited environmental resources. The interaction between rice and planthoppers is modeled using a Holling type II functional response to represent saturation in consumption due to handling time.

The interaction between planthoppers and *Pardosa* sp. is described using the Crowley–Martin functional response, which incorporates predator interference effects that commonly occur in active hunting predators. Combining these assumptions, the ecological interactions are formulated as a system of nonlinear ordinary differential equations as given in Eq. (1). The model is analyzed within the biologically feasible region where all population variables remain positive.

### 2.3. Equilibrium points

The equilibrium points of the model are obtained by setting the time derivatives of all state variables equal to zero. Solving the resulting system yields four equilibrium points, namely the extinction equilibrium, the equilibrium corresponding to the persistence of rice only, the equilibrium representing coexistence of rice and planthoppers in the absence of top predators, and the interior equilibrium where all three populations coexist. When explicit analytical expressions cannot be obtained, equilibrium values are characterized implicitly and later approximated through numerical computation.

### 2.4. Local stability analysis

Local stability of each equilibrium point is investigated by linearizing the system around the equilibrium using the Jacobian matrix. The eigenvalues of the Jacobian matrix determine whether an equilibrium point is stable or unstable. For boundary equilibria, stability conditions are obtained directly from the signs of the eigenvalues. For the interior equilibrium, the characteristic polynomial of the Jacobian matrix is derived and the Routh–Hurwitz criterion is applied to establish sufficient conditions for local asymptotic stability.

### 2.5. Numerical simulation

Numerical simulations are performed to support and illustrate the analytical results. The system of differential equations is solved numerically using positive initial conditions to ensure biological relevance. Several simulation scenarios are considered by varying key biological parameters, particularly the planthopper growth efficiency and the predation intensity of *Pardosa* sp.

Numerical computations and trajectory visualizations are carried out using Python for time integration and plotting, while symbolic computations related to equilibrium analysis and Jacobian derivation are supported by Maple. Phase portraits and time-series plots are used to examine transient dynamics, long-term behavior, and consistency between numerical outcomes and analytical stability results.

## 3. Results and Discussion

This section presents the analytical and numerical results of the three-trophic-level ecological model developed for rice field ecosystems. First, the equilibrium points of the system are identified to describe the possible long-term population states. Next, local stability properties of each equilibrium are analyzed using the Jacobian matrix and the Routh–Hurwitz criterion to determine conditions for stability or instability. The theoretical findings are then supported by numerical simulations under various parameter scenarios, particularly focusing on changes in planthopper growth efficiency and predator predation intensity. Finally, the results are discussed to interpret their ecological implications and to evaluate the role of predator–prey interactions in maintaining rice field ecosystem stability.

### 3.1. Model Formulation

This study develops a three-trophic-level ecological model representing interactions in rice field ecosystems among rice plants (*Oryza sativa*) as producers, brown planthoppers (*Nilaparvata lugens*) as herbivores (primary consumers), and (*Pardosa* sp.) as top predators. Here, the brown planthopper acts as the primary herbivore feeding on rice plants, while *Pardosa* sp. serves as the natural predator regulating the herbivore population. These three components form a nonlinear dynamical system that influences each other through growth, consumption, and predation processes.

The model incorporates two functional responses. The interaction between rice and planthoppers is described by the Holling type II functional response, representing saturation of herbivore consumption due to handling time. The interaction between planthoppers and *Pardosa* sp. is modeled using the Crowley–Martin functional response, which accounts for predator interference effects commonly observed in active hunting predators such as *Pardosa* sp.

Nonlinear predator–prey models with functional responses are widely known to generate rich ecological dynamics, including coexistence and extinction regimes. In particular, the Crowley–Martin functional response has been applied in three-species food chain frameworks to capture predator interference effects and complex trophic interactions [4]. Therefore, the present study aims to develop a biologically realistic three-trophic rice ecosystem model based on these established approaches.

Based on these two response functions, the three-trophic-level ecological model can be written as the following system of differential equations:

$$\begin{aligned}
\frac{dx}{dt} &= rx\left(1-\frac{x}{k}\right)-\frac{qxy}{bx+1},\\
\frac{dy}{dt} &= -sy+\frac{uxy}{bx+1}-\frac{vyz}{efyz+ey+fz+1},\\
\frac{dz}{dt} &= -cz+\frac{wyz}{efyz+ey+fz+1}.
\end{aligned} \tag{1}$$

In the system of differential equations, the rice population is assumed to follow a logistic growth pattern, where the parameter $r$ denotes the intrinsic growth rate of rice and $k$ represents the carrying capacity of the environment. The interaction between rice and planthoppers is modeled using a Holling type II functional response, in which the parameter $q$ denotes the attack rate of planthoppers on rice, while the parameter $b$ represents the handling effect that regulates consumption saturation when rice availability is abundant [19]. The constant term in the denominator ensures saturation at high prey density. The planthopper population is governed by the differential equation for $y$, where the parameter $s$ represents the natural mortality rate of planthoppers, and the parameter $u$ denotes the efficiency of converting consumed rice biomass into planthopper biomass. The interaction between planthoppers and *Pardosa* sp. is described by a Crowley–Martin functional response, in which the parameter $v$ represents the attack rate of *Pardosa* sp. on planthoppers, while the parameters $e$ and $f$ characterize the degree

of predator interference affecting the searching and handling processes, respectively. An increase in predator density is assumed to reduce predation efficiency due to interference among predators. Finally, the parameter $c$ denotes the natural mortality rate of *Pardosa* sp., and the parameter $w$ represents the efficiency of converting consumed planthoppers into predator population growth. All parameters are assumed to be positive, and the initial conditions satisfy $x(0) > 0$, $y(0) > 0$, and $z(0) > 0$.

### 3.2. Positivity and Invariant Region

**Lemma 3.1.** *Suppose $x(0) > 0$, $y(0) > 0$, and $z(0) > 0$. Then the solutions of system (1) remain nonnegative for all $t > 0$.*

*Proof.* On the boundary planes, we have $\frac{dx}{dt}\Big|_{x=0} = 0$, $\frac{dy}{dt}\Big|_{y=0} = 0$, and $\frac{dz}{dt}\Big|_{z=0} = 0$. Therefore, trajectories cannot cross the coordinate planes into the negative region. Thus, $x(t) \geq 0$, $y(t) \geq 0$, and $z(t) \geq 0$ for all $t > 0$, and the nonnegative orthant is positively invariant. □

**Lemma 3.2.** *The rice population is bounded above by the carrying capacity $k$.*

*Proof.* For $x > k$,

$$\frac{dx}{dt} = rx\left(1 - \frac{x}{k}\right) - \frac{qxy}{bx+1} < rx\left(1 - \frac{x}{k}\right) < 0.$$

Therefore, $x(t)$ decreases whenever $x(t) > k$. In particular, if $x(0) \leq k$, then $x(t) \leq k$ for all $t \geq 0$. □

**Lemma 3.3.** *The planthopper and predator populations are bounded.*

*Proof.* From Lemma 2, we have $0 \leq x(t) \leq k$ for all $t \geq 0$. Since

$$D = efyz + ey + fz + 1 \geq 1,$$

the second equation of system (1) gives

$$\dot{y} = -sy + \frac{uxy}{bx+1} - \frac{vyz}{D} \leq -sy + \frac{uxy}{bx+1} \leq -sy + uk\,y = (uk - s)y.$$

Thus, $y(t)$ cannot grow without bound in finite time and remains bounded for biologically relevant solutions. Moreover, the negative predation term ensures that for sufficiently large $y(t)$, the dynamics satisfy $\dot{y} < 0$, preventing unbounded growth and implying ultimate boundedness.
Similarly, from the third equation we obtain

$$\dot{z} = -cz + \frac{wyz}{D} \leq -cz + wyz = z(wy - c).$$

Hence, the predator growth is controlled by the size of the herbivore population. Moreover, whenever $y(t)$ becomes large, the negative predation term $-\frac{vyz}{D}$ in $\dot{y}$ dominates and forces $y(t)$ to decrease, which prevents unbounded growth of $z(t)$.
Therefore, the solutions of system (1) remain in a biologically feasible bounded region. □

### 3.3. Equilibrium points

The equilibrium points is obtained by equating model (1) to 0. This approach is taken because equilibrium can occur when the rate of change in the populations of rice, planthoppers, and *Pardosa* sp. is constant.

$$\frac{dx}{dt} = rx\left(1 - \frac{x}{k}\right) - \frac{qxy}{bx+1} = 0, \tag{2}$$

$$\frac{dy}{dt} = -sy + \frac{uxy}{bx+1} - \frac{vyz}{efyz + ey + fz + 1} = 0, \tag{3}$$

$$\frac{dz}{dt} = -cz + \frac{wyz}{efyz + ey + fz + 1} = 0. \tag{4}$$

Thus, the equilibrium points of system (1) are obtained by solving $\dot{x} = \dot{y} = \dot{z} = 0$. The model admits four equilibrium points as follows.

1. The trivial equilibrium point is
$$E_0 = (0, 0, 0).$$
2. The boundary equilibrium with $y = z = 0$ is obtained from $\dot{x} = 0$, which yields $x = 0$ or $x = k$. Hence, the nontrivial equilibrium is
$$E_1 = (k, 0, 0),$$
representing the survival of rice in the absence of planthoppers and predators.
3. The boundary equilibrium with predator extinction ($z = 0$) is given by
$$E_2 = (x_2, y_2, 0),$$
where $x_2 > 0$ and $y_2 > 0$. From $\dot{y} = 0$ with $z = 0$ we obtain
$$\frac{ux}{bx+1} = s \quad \Rightarrow \quad x_2 = \frac{s}{u - bs}, \qquad u > bs.$$
Substituting $x_2$ into $\dot{x} = 0$ yields
$$y_2 = \frac{r}{q}\left(1 - \frac{x_2}{k}\right)(1 + bx_2).$$
Therefore, $E_2$ exists provided that $u > bs$ and $0 < x_2 < k$ (equivalently $y_2 > 0$).
4. The interior equilibrium point $E_3 = (x^*, y^*, z^*)$ satisfies $x^* > 0$, $y^* > 0$, and $z^* > 0$. From $\dot{x} = 0$, we obtain
$$y^*(x) = \frac{r\left(1 - \frac{x}{k}\right)(1 + bx)}{q}. \tag{E3.1}$$
From $\dot{z} = 0$ (with $z^* > 0$), we have $\dfrac{w\,y^*}{D} = c$, hence
$$D^* = \frac{w}{c}\,y^*, \qquad z^*(y) = \frac{\left(\frac{w}{c} - e\right)y - 1}{f(1 + ey)}. \tag{E3.2}$$
Substituting (E3.1) – (E3.2) into $\dot{y} = 0$ yields an explicit scalar equation
$$F(x) = -s + \frac{ux}{1 + bx} - \frac{v\,z^*(y^*(x))}{D^*(y^*(x))} = 0. \tag{E3.3}$$

Using $D^*(y) = \dfrac{w}{c}y$, we may rewrite $F(x)$ explicitly as

$$F(x) = -s + \frac{ux}{1+bx} - \frac{vc}{wf}\,\frac{\left(\frac{w}{c} - e\right) - \dfrac{1}{y^*(x)}}{1 + e\,y^*(x)}. \tag{E3.4}$$

*Feasibility conditions.* A positive interior equilibrium exists if there is a root $x^* \in (0,k)$ of $F(x) = 0$ such that $y^*(x^*) > 0$ and $z^*(y^*(x^*)) > 0$. Since $y^*(x) > 0$ holds for $0 < x < k$, the positivity of $z^*$ requires

$$\frac{w}{c} > e, \qquad y^*(x^*) > \frac{1}{\frac{w}{c} - e}. \tag{E3.5}$$

In the numerical simulations, the interior equilibrium is approximated numerically by long-time integration of system (1), and the terminal state $(x(T), y(T), z(T))$ for sufficiently large $T$ is taken as an approximation of $(x^*, y^*, z^*)$. Alternatively, for completeness, the root $x^*$ of the scalar equation $F(x) = 0$ can be computed directly using a standard bisection method on the interval $(0, k)$. The iteration is initialized with the endpoints 0 and $k$ and stopped when $|F(x)| < 10^{-8}$. Once $x^*$ is obtained, the corresponding $y^*$ and $z^*$ follow from (E3.1) – (E3.2).

### 3.4. Local stability analysis

To further analyze the dynamics of the three-trophic-level model in rice field ecosystems, a local stability analysis is carried out by evaluating the Jacobian matrix at each equilibrium point. The eigenvalues of the Jacobian matrix are used to determine the local stability of an equilibrium point.

From system (1), define

$$f_1(x,y,z) = rx\left(1 - \frac{x}{k}\right) - \frac{qxy}{bx+1}, \tag{5}$$

$$f_2(x,y,z) = -sy + \frac{uxy}{bx+1} - \frac{vyz}{D}, \tag{6}$$

$$f_3(x,y,z) = -cz + \frac{wyz}{D}, \tag{7}$$

where

$$D = efyz + ey + fz + 1.$$

The Jacobian matrix of system (1) is

$$J(x,y,z) = \begin{pmatrix} r\left(1 - \dfrac{2x}{k}\right) - \dfrac{qy}{(bx+1)^2} & -\dfrac{qx}{bx+1} & 0 \\ \dfrac{uy}{(bx+1)^2} & -s + \dfrac{ux}{bx+1} - \dfrac{vz(fz+1)}{D^2} & -\dfrac{vy(ey+1)}{D^2} \\ 0 & \dfrac{wz(fz+1)}{D^2} & -c + \dfrac{wy(ey+1)}{D^2} \end{pmatrix}.$$

Furthermore, the behavior of solutions around each equilibrium point is described by the following theorems.

**Theorem 3.4.** *The equilibrium point with extinction of all populations $E_0 = (0,0,0)$ is a saddle point.*

*Proof.* At $E_0 = (0, 0, 0)$, we have $bx + 1 = 1$ and $D = 1$, hence

$$J(E_0) = \begin{pmatrix} r & 0 & 0 \\ 0 & -s & 0 \\ 0 & 0 & -c \end{pmatrix}.$$

Therefore, the eigenvalues are

$$\lambda_1 = r, \qquad \lambda_2 = -s, \qquad \lambda_3 = -c.$$

Assuming $r > 0$, $s > 0$, and $c > 0$, one eigenvalue is positive and the other two are negative, so $E_0$ is a saddle point and is unstable. □

**Theorem 3.5.** *The boundary equilibrium point $E_1 = (k, 0, 0)$ is locally asymptotically stable if*

$$\frac{uk}{bk + 1} < s.$$

*Proof.* At $E_1 = (k, 0, 0)$, we obtain

$$J(E_1) = \begin{pmatrix} -r & -\dfrac{qk}{bk+1} & 0 \\ 0 & -s + \dfrac{uk}{bk+1} & 0 \\ 0 & 0 & -c \end{pmatrix}.$$

Hence, the eigenvalues are

$$\lambda_1 = -r, \qquad \lambda_2 = -s + \frac{uk}{bk + 1}, \qquad \lambda_3 = -c.$$

Since $r > 0$ and $c > 0$, we have $\lambda_1 < 0$ and $\lambda_3 < 0$. Thus, $E_1$ is locally asymptotically stable if and only if $\lambda_2 < 0$, i.e.,

$$-s + \frac{uk}{bk + 1} < 0 \quad \Longleftrightarrow \quad \frac{uk}{bk + 1} < s.$$

□

**Theorem 3.6.** *The boundary equilibrium point $E_2 = (x_2, y_2, 0)$ is locally asymptotically stable if*

$$\lambda_3 < 0, \qquad \mathrm{tr}(J_{xy}) < 0, \qquad \det(J_{xy}) > 0,$$

*where $\lambda_3$ is the eigenvalue associated with the predator direction and $J_{xy}$ denotes the $2 \times 2$ Jacobian submatrix corresponding to the $(x, y)$-subsystem at $E_2$.*

*Proof.* At $E_2 = (x_2, y_2, 0)$, we have $D = ey_2 + 1$ and the Jacobian becomes block triangular. The eigenvalue associated with the predator direction is

$$\lambda_3 = -c + \frac{wy_2}{ey_2 + 1}.$$

The remaining two eigenvalues are determined by the characteristic equation of the $2 \times 2$

block

$$J_{xy}(E_2) = \begin{pmatrix} a_{11} & a_{12} \\ a_{21} & a_{22} \end{pmatrix},$$

where

$$a_{11} = r\left(1 - \frac{2x_2}{k}\right) - \frac{qy_2}{(bx_2+1)^2}, \qquad a_{12} = -\frac{qx_2}{bx_2+1},$$
$$a_{21} = \frac{uy_2}{(bx_2+1)^2}, \qquad a_{22} = -s + \frac{ux_2}{bx_2+1}.$$

Since $E_2$ satisfies $\dot{y} = 0$ with $z = 0$, we have

$$\frac{ux_2}{bx_2+1} = s \quad \Rightarrow \quad a_{22} = 0.$$

Thus,

$$\mathrm{tr}(J_{xy}) = a_{11} + a_{22} = a_{11}, \qquad \det(J_{xy}) = a_{11}a_{22} - a_{12}a_{21} = -a_{12}a_{21} > 0,$$

because $a_{12} < 0$ and $a_{21} > 0$. Therefore, the two eigenvalues of $J_{xy}(E_2)$ have negative real parts if and only if $\mathrm{tr}(J_{xy}) < 0$ and $\det(J_{xy}) > 0$. Together with $\lambda_3 < 0$, this yields the stated stability conditions. □

**Theorem 3.7.** *Suppose $E_3 = (x^*, y^*, z^*)$ is an interior equilibrium point of system (1) with $x^* > 0$, $y^* > 0$, and $z^* > 0$. Let $J(E_3) = [a_{ij}]_{3\times 3}$ denote the Jacobian matrix evaluated at $E_3$. The characteristic polynomial of $J(E_3)$ is*

$$\det(\lambda I - J(E_3)) = \lambda^3 + A_1\lambda^2 + A_2\lambda + A_3,$$

*where*

$$A_1 = -(a_{11} + a_{22} + a_{33}),$$
$$A_2 = a_{11}a_{22} + a_{11}a_{33} + a_{22}a_{33} - a_{12}a_{21} - a_{23}a_{32},$$

*and*

$$A_3 = -\det(J(E_3)) = -a_{11}(a_{22}a_{33} - a_{23}a_{32}) + a_{12}a_{21}a_{33}.$$

*Then, $E_3$ is locally asymptotically stable if and only if*

$$A_1 > 0, \qquad A_2 > 0, \qquad A_3 > 0, \qquad A_1A_2 > A_3.$$

*Proof.* The above coefficients are obtained from the characteristic polynomial of $J(E_3)$. By the Routh–Hurwitz criterion for cubic polynomials, all roots of $\lambda^3 + A_1\lambda^2 + A_2\lambda + A_3 = 0$ have negative real parts if and only if

$$A_1 > 0, \qquad A_2 > 0, \qquad A_3 > 0, \qquad A_1A_2 > A_3.$$

This is equivalent to the local asymptotic stability of the equilibrium point $E_3$. □

### 3.5. Numerical simulation

All numerical simulations were performed in Python (Google Colab) using the `solve_ivp` routine from `scipy.integrate` with the explicit Runge–Kutta method of order (4,5) (`RK45`). The system was integrated on the time interval $t \in [0, 500]$ using a uniform output grid of 6000 points. The relative and absolute tolerances were set to `rtol` $= 10^{-7}$ and `atol` $= 10^{-9}$ to ensure numerical

accuracy.

For all scenarios, the same positive initial conditions were used: $(x(0), y(0), z(0)) = (2.0, 1.0, 0.5)$.

Scenario (A) uses the baseline parameter set in Table 1. In Scenario (B), the predation intensity was increased from $v = 1.5$ to $v = 8.0$ and the predator mortality rate was decreased from $c = 0.01$ to $c = 0.005$ to produce a near-extinction outcome for the planthopper population. In Scenario (C), the predator mortality rate was increased from $c = 0.01$ to $c = 0.2$ to produce predator extinction. All remaining parameters were kept identical to the baseline values reported in Table 1.

**Table 1:** Parameter values

| Parameter | Values | Source |
|---|---|---|
| $r$ | 1.55 | [19] |
| $k$ | 6 | [19] |
| $w$ | 1 | [20] |
| $b$ | 1.3 | Assumption |
| $s$ | 0.4 | [19] |
| $e$ | 2 | [17] |
| $f$ | 2.5 | Assumption |
| $c$ | 0.01 | Assumption |
| $u$ | 2.4 | Assumption |
| $v$ | 1.5 | Assumption |
| $q$ | 2.0 | Assumption |

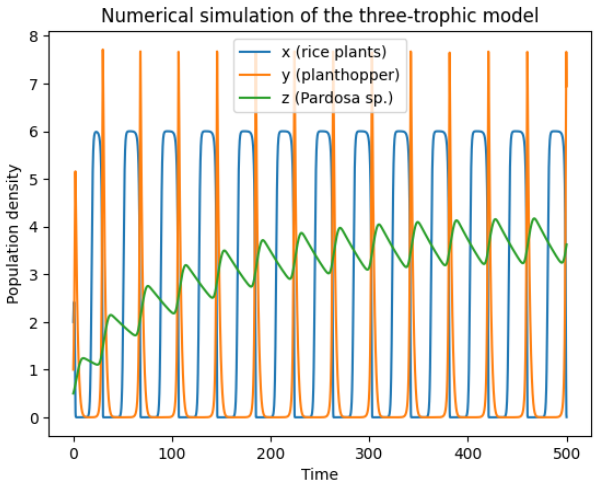


**Figure 1:** Time series of rice plant ($x$), planthopper ($y$), and *Pardosa* sp. ($z$) populations generated by the three-trophic ecological model using the parameter values listed in Table 1.

Fig. 1 illustrates the temporal evolution of the three populations under the parameter values given in Table 1. The rice plant ($x$), planthopper ($y$), and *Pardosa* sp. ($z$) densities remain positive for all time, indicating biological feasibility of the solution within rice field ecosystems. The trajectories exhibit sustained oscillatory behavior, reflecting recurrent predator–prey interactions across trophic levels. In particular, fluctuations in the planthopper population are regulated by predation pressure from *Pardosa* sp., while the rice plant population recovers as herbivore density decreases. This dynamic outcome suggests that variations in ecological parameters may significantly influence the long-term balance between coexistence and population decline in rice field ecosystems.

To further illustrate the long-term dynamics of system (1), three-dimensional phase portraits are presented under different parameter scenarios. These phase trajectories provide a geometric interpretation of the convergence behavior toward boundary or interior equilibrium points.

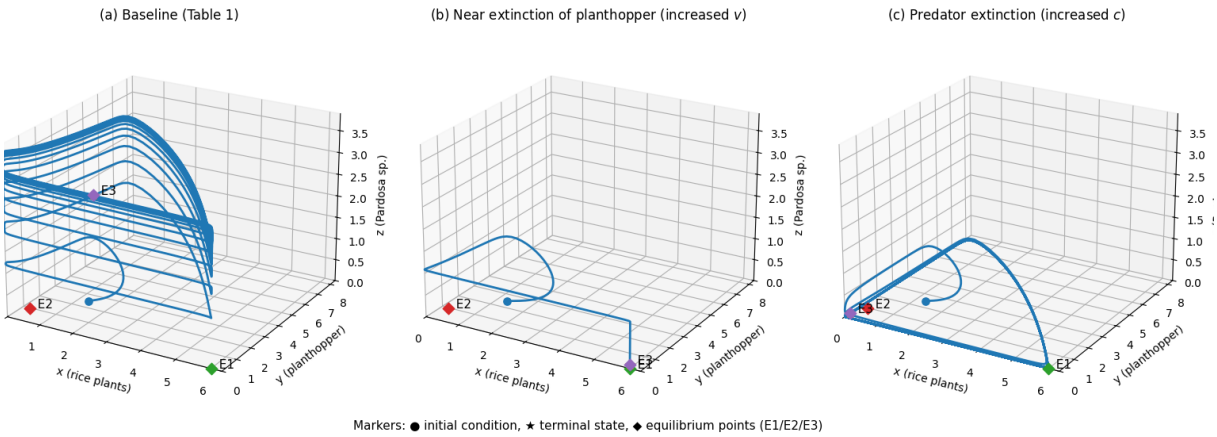


**Figure 2:** Three-dimensional phase portraits of the three-trophic rice ecosystem model: (a) baseline coexistence equilibrium under Table 1 parameters, (b) near extinction of the planthopper population under increased predation intensity, and (c) predator extinction under increased predator mortality.Markers indicate the initial state (●), terminal state (⋆), and equilibrium points (⧫).

Fig. 2 provides a geometric illustration of the system trajectories under three different ecological scenarios. In the baseline case (Fig. 2(a)), the solution converges toward the interior equilibrium point $E_3$, indicating stable coexistence of rice, planthoppers, and *Pardosa* sp. populations, which is consistent with the analytical stability condition given in Theorem 4.

When the predation intensity of *Pardosa* sp. is increased (Fig. 2(b)), the planthopper population declines to a very low level, representing a near-extinction state, while the predator persists. This demonstrates that stronger top–down predation pressure may suppress herbivore outbreaks and shift the long-term balance of the ecosystem.

In contrast, increasing the predator mortality rate leads to predator extinction (Fig. 2(c)), where trajectories approach the boundary equilibrium point $E_2$. In this case, the predator population vanishes and the system reduces to a producer–herbivore interaction. These numerical phase portraits confirm that small variations in biological parameters can significantly alter the stability structure of the three-trophic rice ecosystem model.

Although a complete bifurcation analysis is beyond the scope of this study, the numerical experiments indicate that threshold values of key parameters may separate regimes of coexistence and extinction. In particular, changes in the predation intensity $v$ and the predator mortality rate $c$ can shift the long-term dynamics from a stable interior equilibrium to boundary equilibria associated with population collapse. A more systematic bifurcation and sensitivity investigation would be an important direction for future work to better quantify these transition mechanisms.

To provide a clearer numerical interpretation of the analytical stability results, several simulation scenarios were examined under different ecological conditions. Using the baseline parameter set in Table 1, the system exhibits stable coexistence among rice, planthoppers, and *Pardosa* sp. However, when key parameters related to predation intensity and predator mortality are varied, the long-term dynamics may shift toward extinction states. A summary of the numerical scenarios considered in this study is presented in Table 2.

**Table 2:** Parameter scenarios used in the numerical simulations.

| Scenario | Description | Varied parameter(s) | Long-term outcome |
|---|---|---|---|
| (A) | Baseline coexistence (Table 1) | Default values: $v = 1.5, c = 0.01$ | Stable interior equilibrium $E_3$. |
| (B) | Near extinction of the planthopper population | Increased predation intensity: $v$ : $1.5 \to 8.0$<br>Decreased predator mortality: $c$ : $0.01 \to 0.005$ | $y(t) \to 0$ (herbivore suppression). |
| (C) | Predator extinction | $c : 0.01 \to 0.2$ | $z(t) \to 0$ (boundary equilibrium $E_2$). |

Table 2 summarizes the three numerical simulation scenarios considered in this study in order to illustrate the qualitative behaviors predicted by the analytical stability results. Scenario (A) corresponds to the baseline parameter set in Table 1, where the three populations coexist and trajectories converge to the stable interior equilibrium $E_3$. Scenario (B) explores the effect of stronger predation pressure by increasing the attack rate $v$, leading to a near-extinction state of the planthopper population. Scenario (C) investigates predator extinction by increasing the predator mortality rate $c$, causing solutions to approach the boundary equilibrium $E_2$. These scenarios highlight how variations in key ecological parameters may shift the long-term outcomes between coexistence and extinction regimes.

## 4. Conclusion

In this paper, a three-trophic rice field ecosystem model was proposed by combining the Holling type II functional response for the rice–planthopper interaction and the Crowley–Martin functional response for the planthopper–predator interaction. The model captures not only the saturation effect in herbivore consumption, but also predator interference at the upper trophic level.

The analysis shows that the system admits several equilibrium points, including boundary equilibria associated with extinction outcomes and an interior equilibrium representing coexistence of rice, planthoppers, and *Pardosa* sp. Local stability conditions were derived through the Jacobian matrix together with the Routh–Hurwitz criterion, providing analytical insight into when coexistence can persist.

Numerical experiments were consistent with the theoretical results. In particular, changes in key ecological parameters such as predation intensity and predator mortality were observed to shift the long-term dynamics from stable coexistence toward near-extinction or predator collapse scenarios.

It is important to emphasize that the present study remains theoretical in nature. Several parameter values were selected based on reasonable assumptions rather than direct calibration from field observations, and factors such as seasonal variation or spatial effects were not included. Further work could therefore focus on parameter estimation using empirical data, as well as sensitivity or bifurcation investigations to better understand transitions between ecological regimes.

## CRediT Authorship Contribution Statement

**Anastasya Choirun Nisa':** Conceptualization, methodology, formal analysis, investigation, resources, data curation, and writing original draft preparation, writing review and editing. **Dian Savitri:** Conceptualization, methodology, software, validation, writing review and editing, visualization, and supervision.

## Declaration of Generative AI and AI-assisted technologies

Generative AI tools (specifically ChatGPT) were used in a limited manner to assist with language refinement, grammar checking, and improvement of academic writing clarity during the manuscript preparation. In addition, AI-based translation support (DeepL) was utilized to assist in translating and aligning the manuscript into proper academic English. All research design, mathematical modeling, analytical derivations, numerical simulations, result interpretation, and scientific conclusions were entirely conceived, performed, and written by the authors. No generative AI tools were used to generate the core scientific content or research findings.

## Declaration of Competing Interest

The authors declare no competing interests.

## Funding and Acknowledgments

This research received no external funding.

## Data and Code Availability

No experimental or observational datasets were generated or analysed in this study. All parameter values used in the numerical simulations were obtained from the cited literature or defined as model assumptions, as described in the manuscript. The simulation codes are available from the corresponding author upon reasonable request.

## References

[1] W. Kong and Y. Shao, "The effects of fear and delay on a predator-prey model with crowley-martin functional response and stage structure for predator," *AIMS Mathematics*, vol. 8, no. 12, pp. 29 260–29 289, 2023. DOI: 10.3934/math.20231498.

[2] N. E. Papanikolaou, T. Kypraios, H. Moffat, A. Fantinou, D. P. Perdikis, and C. Drovandi, "Predators' functional response: Statistical inference, experimental design, and biological interpretation of the handling time," *Frontiers in Ecology and Evolution*, vol. 9, p. 740 848, 2021. DOI: 10.3389/fevo.2021.740848.

[3] A. N. Salsabila and D. Savitri, "Dynamical analysis of holling tanner prey predators model with add food in second level predators," *Jambura Journal of Biomathematics*, vol. 5, no. 2, 2024. DOI: 10.37905/jjbm.v5i2.25753.

[4] R. K. Upadhyay and R. K. Naji, "Dynamics of a three species food chain model with crowley–martin type functional response," *Chaos, Solitons & Fractals*, vol. 42, no. 3, pp. 1337–1346, 2009. DOI: 10.1016/j.chaos.2009.03.020.

[5] K. S. Reddy, K. L. Narayan, and N. C. P. Ramacharyulu, "A three species ecosystem consisting of a prey, predator and super predator," *Mathematics Applied in Science and Technology*, vol. 2, no. 1, pp. 95–107, 2010.

[6] D. Savitri and H. S. Panigoro, "Bifurkasi hopf pada model prey–predator–super predator dengan fungsi respon yang berbeda," *Jambura Journal of Biomathematics*, vol. 1, no. 2, pp. 65–70, 2020. DOI: 10.34312/jjbm.v1i2.8399.

[7] C. Wang, W. Zhu, and A. Szolnoki, "The conflict between self-interaction and updating passivity in the evolution of cooperation," *Chaos, Solitons & Fractals*, vol. 173, p. 113 667, 2023. DOI: 10.1016/j.chaos.2023.113667.

[8] C. S. Holling, "The components of predation as revealed by a study of small-mammal predation of the european pine sawfly," *The Canadian Entomologist*, vol. 91, no. 5, pp. 293–320, 1959. DOI: 10.4039/Ent91293-5.

[9] N. L. Aufaniyah and A. Abadi, "Dynamics of prey–predator interaction with type ii holling response function, additional food, and anti-predator behavior," *Mathunesa Journal*, vol. 11, no. 3, pp. 422–433, 2023. DOI: 10.26740/mathunesa.v11n3.p422-433.

[10] J. D. Murray, *Mathematical Biology I: An Introduction*, 3rd. New York: Springer, 2002.

[11] M. Kot, *Elements of Mathematical Ecology*. Cambridge: Cambridge University Press, 2001.

[12] J. Mo, W. Li, D. He, S. Wang, and X. Zhou, "Dynamic Analysis of a Predator–Prey Model with Holling-II Functional Response," *Journal of Applied Mathematics and Physics*, vol. 11, no. 10, 2023. DOI: 10.4236/jamp.2023.1110188.

[13] S. Wang, H. Yu, C. Dai, and M. Zhao, "The dynamical behavior of a certain predator–prey system with holling type ii functional response," *Journal of Applied Mathematics and Physics*, vol. 8, no. 3, 2020. DOI: 10.4236/jamp.2020.83042.

[14] D. A. Fitri and D. Savitri, "Prey predator model with holling type ii functional response and hunting cooperation of predators," *MATHunesa: Jurnal Ilmiah Matematika*, vol. 12, no. 3, pp. 637–645, 2024. DOI: 10.26740/mathunesa.v12n3.p637-645.

[15] P. H. Crowley and E. K. Martin, "Functional responses and interference within and between year classes of a dragonfly population," *Journal of the North American Benthological Society*, vol. 8, no. 3, pp. 211–221, 1989. DOI: 10.2307/1467324.

[16] J. R. Beddington, "Mutual interference between parasites or predators and its effect on searching efficiency," *Journal of Animal Ecology*, vol. 44, no. 1, pp. 331–340, 1975. DOI: 10.2307/3866.

[17] R. D. Parshad, A. Basheer, D. Jana, and J. P. Tripathi, "Do prey handling predators really matter: Subtle effects of a crowley–martin functional response," *Chaos, Solitons & Fractals*, vol. 103, pp. 410–421, 2017. DOI: 10.1016/j.chaos.2017.06.027.

[18] Miswanto, N. Suroiyah, and Windarto, "Model Predator–Prey Leslie-Gower dengan Respon Crowley-Martin dan Prey Terinfeksi serta Faktor Ketakutan," *Limits: Journal of Mathematics and Its Applications*, vol. 20, no. 3, pp. 331–342, 2023. DOI: 10.12962/limits.v20i3.18530.

[19] J. Alebraheem, "Predator interference in a predator–prey model with mixed functional and numerical responses," *Journal of Mathematics*, vol. 2023, pp. 1–13, 2023. DOI: 10.1155/2023/4349573.

[20] J. Alebraheem, "Rich dynamics of seasonal carrying capacity prey–predator models with crowley–martin functional response," *Mathematical and Computational Applications*, vol. 30, no. 1, p. 11, 2025. DOI: 10.3390/mca30010011.